

**Understanding of
Materials State and its Degradation
using
Non-Linear Ultrasound (NLU) Approaches**

PROJECT REPORT

Period Jan-Jul 2011

**Submitted to
AOARD
AFOSR
Tokyo, Japan**

**Principal Investigator
Dr. Krishnan Balasubramaniam
Department of Mechanical Engineering and
Centre for Nondestructive Evaluation
Indian Institute of Technology Madras, Chennai, 600 036
Tele: +91-44-2257-4662
Fax: +91-44-2257-0545
Email: balas@iitm.ac.in**

July 2011



Report Documentation Page

Form Approved
OMB No. 0704-0188

Public reporting burden for the collection of information is estimated to average 1 hour per response, including the time for reviewing instructions, searching existing data sources, gathering and maintaining the data needed, and completing and reviewing the collection of information. Send comments regarding this burden estimate or any other aspect of this collection of information, including suggestions for reducing this burden, to Washington Headquarters Services, Directorate for Information Operations and Reports, 1215 Jefferson Davis Highway, Suite 1204, Arlington VA 22202-4302. Respondents should be aware that notwithstanding any other provision of law, no person shall be subject to a penalty for failing to comply with a collection of information if it does not display a currently valid OMB control number.

1. REPORT DATE 12 AUG 2011		2. REPORT TYPE		3. DATES COVERED	
4. TITLE AND SUBTITLE Understanding of Materials State and its Degradation using Non-Linear Ultrasound (NLU) Approaches				5a. CONTRACT NUMBER	
				5b. GRANT NUMBER	
				5c. PROGRAM ELEMENT NUMBER	
6. AUTHOR(S) Krishnan Balasubramaniam				5d. PROJECT NUMBER	
				5e. TASK NUMBER	
				5f. WORK UNIT NUMBER	
7. PERFORMING ORGANIZATION NAME(S) AND ADDRESS(ES) Department of Aerospace Engineering, IIT Madras, Bangalore 5670 012, India, NA, NA				8. PERFORMING ORGANIZATION REPORT NUMBER N/A	
9. SPONSORING/MONITORING AGENCY NAME(S) AND ADDRESS(ES)				10. SPONSOR/MONITOR'S ACRONYM(S)	
				11. SPONSOR/MONITOR'S REPORT NUMBER(S)	
12. DISTRIBUTION/AVAILABILITY STATEMENT Approved for public release; distribution unlimited.					
13. SUPPLEMENTARY NOTES					
14. ABSTRACT Nonlinear ultrasonic (NLU) harmonic generation to a harmonic wave amplitude input has been simulated in 1D and in 2D using a Mass Spring Lattice Model (MSLM). Previously a Finite Difference Time Domain (FDTD) model was developed in this project. The MSLM model is expected to have improved application for the modeling of the nonlinear behavior of the ultrasonic wave propagation in isotropic and anisotropic materials systems. The 1D MSLM model was developed and the NLU behavior has been simulated and verified using previously reported data. The incorporation of the nonlinear parameters in the 2-D model is currently underway.					
15. SUBJECT TERMS					
16. SECURITY CLASSIFICATION OF:			17. LIMITATION OF ABSTRACT	18. NUMBER OF PAGES 34	19a. NAME OF RESPONSIBLE PERSON
a. REPORT unclassified	b. ABSTRACT unclassified	c. THIS PAGE unclassified			

ABSTRACT

Key words: Nonlinear ultrasonic technique, Second harmonic generation, nonlinear wave equation, static displacement, Mass Spring Lattice Model (MSLM).

Nonlinear ultrasonic harmonic generation to an input harmonic wave amplitude has been simulated first in 1D and then subsequently in 2D using an Mass Spring Lattice Model (MSLM). This is augment to the earlier developed Finite Difference Time Domain (FDTD) model in this project. The MSLM model is expected to have improved application for the modeling of the Non-Linear behavior of the ultrasonic wave propagation in isotropic and anisotropic materials systems. The 1-D MSLM model was developed and the NLU behavior has been simulated and verified using previously reported data. The 2-D MSLM model has also been developed and verified for Linear ultrasonic wave propagation using commercial FEM package. The incorporation of the non-linear parameters in the 2-D model is currently underway.

LIST OF SYMBOLS

A_1	Amplitude of fundamental frequency
A_2	Amplitude of second harmonic frequency
A_{dc}	Static Displacement
ω	Angular frequency
β	Nonlinearity Parameter
dt	Time step size
h	Space step size
z	Distance of propagation
σ	Stress
ε	Strain
ρ	Density of material
E	Elastic modulus
u_t^i	Displacement of the particle at the i^{th} node at time t .

CONTENTS

LIST OF SYMBOLS	iii
1.1 INTRODUCTION	2
1.2 MASS SPRING LATTICE MODEL – 1 D.....	2
1.2.1 Comparison with Cantrell’s theory:.....	5
1.3 ASYMMETRY AND THE STATIC DISPLACEMENT COMPONENT GENERATION	7
1.3.1 Dependence of the static displacement component on various input parameters	14
1.4 2D ULTRASONIC WAVE PROPAGATION MODEL FOR MSLM	18
1.5 THE 2D MSLM MODEL	19
1.6 2D MSLM SIMULATION RESULTS USING MATLAB.....	22
1.7 COMPARISON WITH COMMERCIAL FEM SOFTWARE (ABAQUS). ...	25
1.8 FUTURE WORK IN 2D MSLM MODELLING	28
1.9 REFERENCES.....	28

1.1 INTRODUCTION

This report deals with the simulation of the finite amplitude ultrasonic wave propagation in materials with accumulated no nonlinearity. The wave propagation is simulated by solving the wave equation with the constitutive behavior of the nonlinear medium. It is proved that an asymmetric stress strain relationship of the material resulting from asymmetric motion of the dislocations is required for the generation of the second harmonic and the static displacement component while the third harmonic is generated even if the stress strain relation is symmetric. The dependencies of the generated static displacement and the second harmonic on various input parameters are evaluated and are compared with the existing literature. The simulation is carried out using a mass spring lattice model based finite difference time domain approach.

1.2 MASS SPRING LATTICE MODEL – 1 D

The Mass Spring Lattice model is an invaluable tool for simulating wave propagation and has been successfully used for visualizing waves propagating through complex media. The MSLM model for simulating a finite amplitude ultrasonic wave propagation through a material is based on the following assumptions. (Holland 2002)

- (a) The specimen is a collection of n mass points each of mass m
- (b) The mass points are connected by classical nonlinear springs
- (c) The force displacement relation of the classical nonlinear spring till the third order is given by

$$F_i = k_1 x_i + \frac{1}{2} k_2 x_i^2 + \frac{1}{3} k_3 x_i^3 \quad \dots\dots\dots(1)$$

where F_i is the force and x_i is the elongation/compression in the spring.

The following are the terms used in the derivation

m = mass of each mass particle

u_t^i = displacement of the particle at the i -th node at time t .

Δt = time step

Δx = distance between two consecutive mass points

ρ = density of the material

E = Modulus of elasticity of the material (Second order elastic constant)

β = Second order nonlinearity parameter of the material.

A = area of cross section (assumed uniform)

γ = Third order nonlinearity parameter of the material.

Applying Newton's Second Law of motion for the i -th mass we would have

$$m \frac{d^2 u_i}{dt^2} = [k_1 (u_{i+1}^t - u_i^t) + \frac{1}{2} k_2 (u_{i+1}^t - u_i^t)^2 + \frac{1}{3} k_3 (u_{i+1}^t - u_i^t)^3] - [k_1 (u_i^t - u_{i-1}^t) + \frac{1}{2} k_2 (u_i^t - u_{i-1}^t)^2 + \frac{1}{3} k_3 (u_i^t - u_{i-1}^t)^3] \quad (2)$$

i.e.

$$\begin{aligned}
m \frac{u_i^{t+\Delta t} - 2u_i^t + u_i^{t-\Delta t}}{(\Delta t)^2} &= [k_1(u_{i+1}^t - 2u_i^t + u_{i-1}^t) + \frac{1}{2}k_2(u_{i+1}^t - 2u_i^t + u_{i-1}^t)(u_{i+1}^t - u_{i-1}^t) \\
&+ \frac{1}{3}k_3((u_{i+1}^t - 2u_i^t + u_{i-1}^t)((u_{i+1}^t - u_i^t)^2 + (u_{i+1}^t - u_i^t)(u_i^t - u_{i-1}^t) \\
&+ (u_i^t - u_{i-1}^t)^2)]
\end{aligned}$$

(3)

The above equation (3) has only one term $u_i^{t+\Delta t}$ referring to the future time and hence can be iterated in time to yield the displacement matrix $u(i,t)$ Re-arranging the above equation we have

$$\begin{aligned}
u_i^{t+\Delta t} &= 2u_i^t - u_i^{t-\Delta t} \frac{(\Delta t)^2}{m} [k_1(u_{i+1}^t - 2u_i^t + u_{i-1}^t) + \frac{1}{2}k_2(u_{i+1}^t - 2u_i^t + u_{i-1}^t)(u_{i+1}^t - u_{i-1}^t) \\
&+ \frac{1}{3}k_3((u_{i+1}^t - 2u_i^t + u_{i-1}^t)((u_{i+1}^t - u_i^t)^2 + (u_{i+1}^t - u_i^t)(u_i^t - u_{i-1}^t) + (u_i^t - u_{i-1}^t)^2)] \quad \dots \quad (4)
\end{aligned}$$

The above equation (4) can be used to evaluate the displacements at all the nodes given the initial and boundary conditions Making dx and dt tend to zero in the (3.3) and comparing it with the wave equation in continuous form i.e.

$$\rho \frac{\partial^2 u}{\partial t^2} = E \frac{\partial^2 u}{\partial x^2} (1 - 2\beta \frac{\partial u}{\partial x} - 3\gamma \left(\frac{\partial u}{\partial x} \right)^2) \quad (5)$$

and using $m = \rho A \Delta x$, provides the following,

$$k_1 = \frac{EA}{\Delta x}, k_2 = \frac{2E\beta A}{\Delta x^2}, k_3 = \frac{3E\gamma A}{\Delta x^3}$$

The values of Δx and Δt are chosen to avoid dispersion (as suggested by Holland,2002).

A Hanning windowed sinusoidal pulse was used as input to the simulations conducted using the above formulation. A Matlab® code was utilized to simulate the wave propagation using the FDTD equations discussed in the previous section.

The simulations are validated against Cantrell's (1984, 1987).theory for generation of static displacement component

1.2.1 Comparison with Cantrell's theory:

Yost and Cantrell (1987) developed an expression for the static strain generated when a wave propagates through a material with accumulated nonlinearities

The equation reads as

$$\frac{\partial u}{\partial x} = -\frac{1}{c_0} \frac{\partial u}{\partial t} + \frac{\beta}{2c_0^2} \left(\frac{\partial u}{\partial t} \right)^2 \quad (6)$$

Where x is along the direction of propagation of wave $u(x,t)$ denotes the displacement at the coordinate x at time t . The static strain component is given by the time average of $\frac{\partial u}{\partial x}$

Taking time average on both the sides of equation (6) we get

$$\left\langle \frac{\partial u}{\partial x} \right\rangle = -\frac{1}{c_0} \left\langle \frac{\partial u}{\partial t} \right\rangle + \frac{\beta}{2c_0^2} \left\langle \left(\frac{\partial u}{\partial t} \right)^2 \right\rangle \quad (7)$$

The right hand side of the above equation (7) is estimated by taking the averages of

$\left(\frac{\partial u}{\partial t} \right)^2$ and $\left(\frac{\partial u}{\partial t} \right)$ from the simulated $u(x,t)$ profiles and then evaluating the integral in

the above equation (7). The obtained values are compared with the static displacement obtained from the simulated displacement wave's Fast Fourier Transform. This was performed for different values of frequency, input amplitude, nonlinearity parameter of

the material and propagation distance. One such comparison is shown in Table 1. The results show excellent agreement between the published data and the simulated data using the FDTD MSLM model reported here. The maximum difference between the two results observed only in the second decimal and can be attributed to the numerical errors during the computation.

The simulations are further verified by comparing variation of the generated harmonic with the distance of propagation, input amplitude and the frequency of the input wave. It has been found to comply with the well-known relation

$$A_2 \propto \beta A_1^2 k^2 x \quad (8)$$

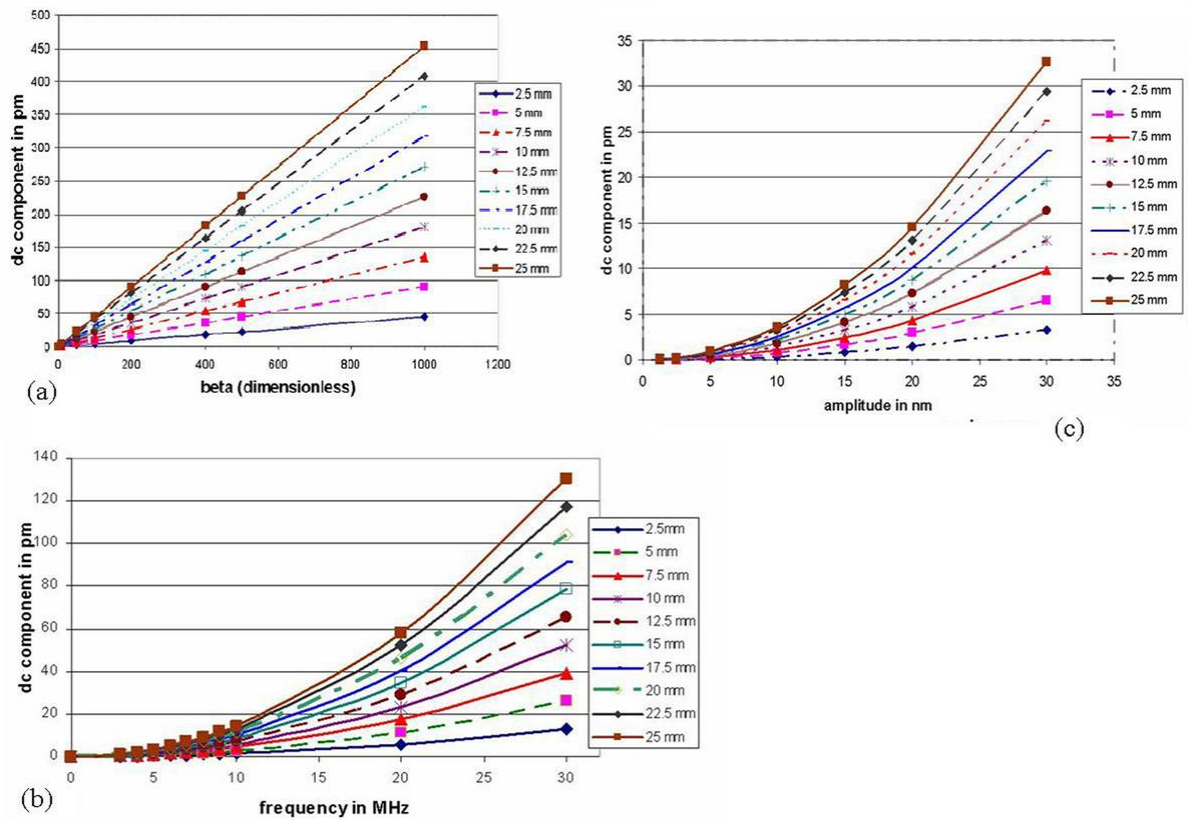


Fig 1 shows the variation of the second harmonic with the various input parameters- the nonlinearity parameter, input amplitude, frequency of the wave and the distance of propagation.

1.3 ASYMMETRY AND THE STATIC DISPLACEMENT COMPONENT GENERATION

To explore the dependence of the static displacement component and the second harmonic on the stress strain relation of the material, the above simulations are carried out for the following two cases

- I. $\beta = 0, \gamma \neq 0$ (symmetric stress strain relationship)

II. $\beta \neq 0, \gamma = 0$ (asymmetric stress relationship)

Case I:

In this case the stress-strain relationship of the material is taken in the following form

$$\sigma = E(\varepsilon - \gamma\varepsilon^3) \quad (3.9)$$

Where γ is the third order nonlinearity of the material.

Fig 2 shows a plot of the simulated time domain signal of the wave obtained after a distance of propagation of 25 mm. If the signal is compared with the input wave it is observed that the symmetry of the wave is restored. In other words, the positive half cycle and the negative half cycle distort in a similar way. The stress strain plot for this case is as shown in Fig 3. It may be seen that the stress strain curve has point symmetry about the origin. Thus it can be concluded that such a symmetric stress strain relationship of the damaged material implies that the distorted signal restores its symmetry after propagation.

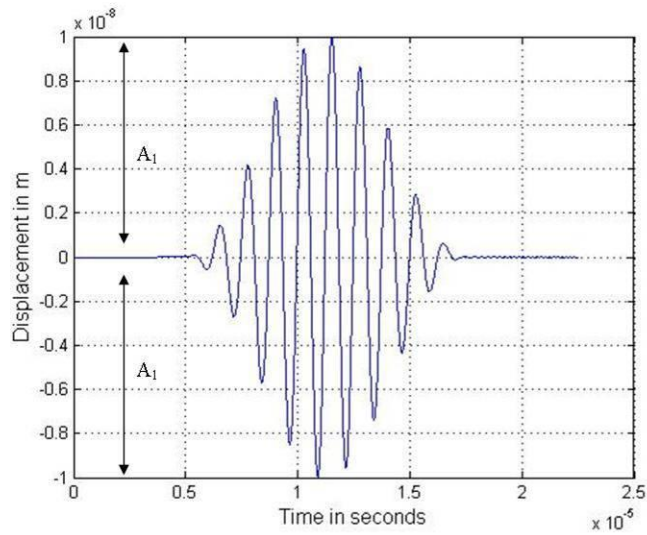


Fig 2. Wave after a propagation of 25 mm for Case I.

To obtain the frequency spectrum, the FFT routines in Matlab were employed on the time domain signals, for different distances of wave propagation. Fig 4 shows the FFTs of the wave after different distances of propagation. It can be seen that no static displacement component is generated in this case, and only the odd harmonics are generated.

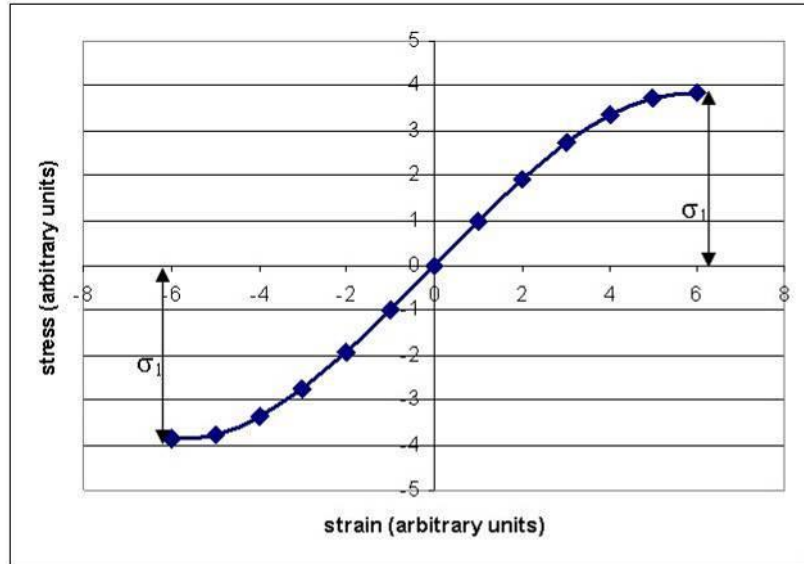


Fig 3 A symmetric stress strain curve

Case II:

In this case the stress-strain relationship of the material is taken in the following form

$$\sigma = E(\varepsilon - \beta\varepsilon^2) \quad (10)$$

Where β is the second order nonlinearity of the material.

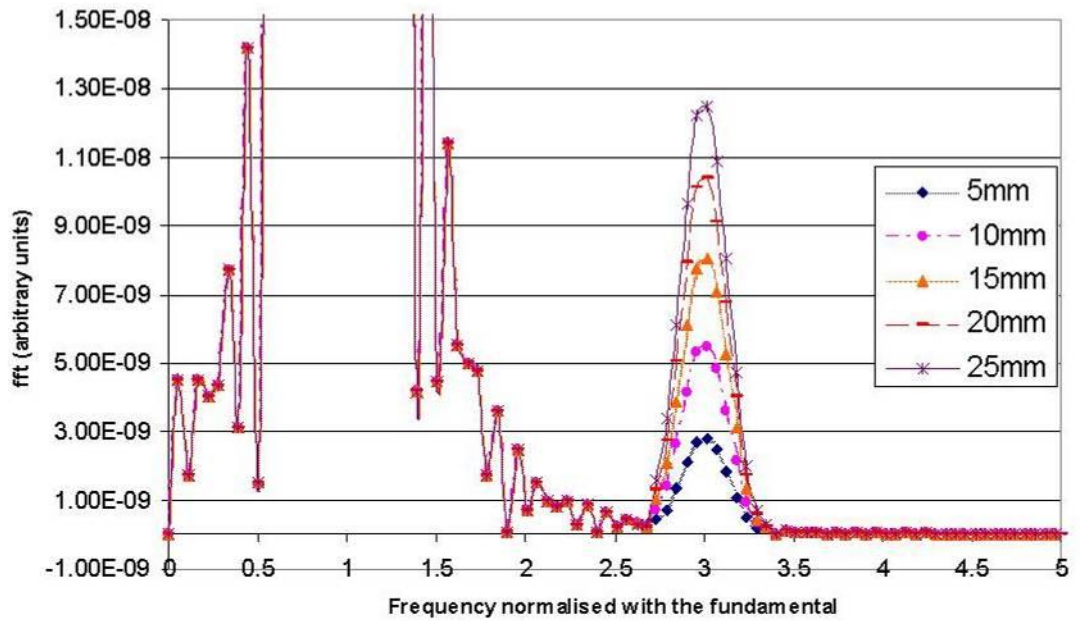


Fig 4 . FFT of the propagated wave for Case I after different distances of propagation showing no generated static displacement component.

Fig 5 shows a plot of the simulated time domain signal of the wave obtained after a distance of propagation of 25 mm. If the transmitted signal is compared with the input signal, an asymmetry induced into the wave could be observed in the time domain, i.e. the positive half cycle and the negative half cycle don't distort the same way. The stress-strain plot for this case is as shown in Fig 6. It may be seen that the corresponding stress-strain curve is also asymmetric for this case.

Fig 7 shows the FFTs of the wave after different distances of propagation for Case II material. It can be seen that a static displacement component increases with the distance of propagation. Also both even and odd harmonics were generated, as expected.

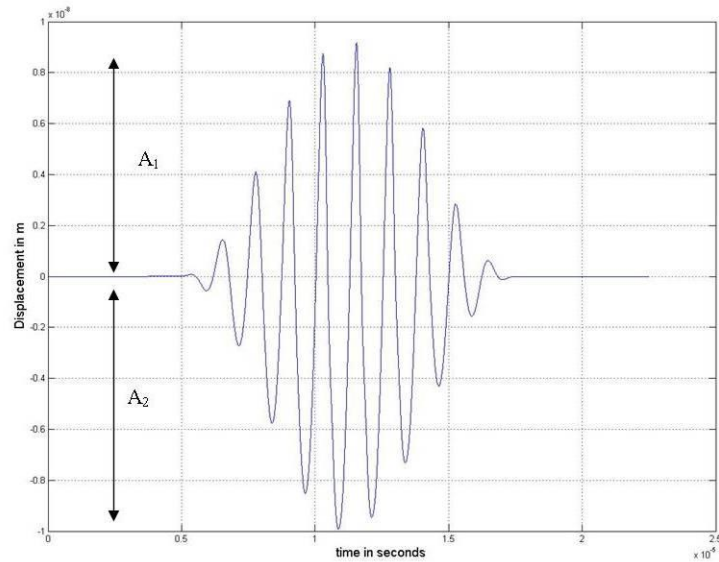


Fig 5. Wave after a propagation of 25 mm for Case II.

Oruganti et al (2007) have shown that an asymmetry in the stress-strain curve of the material which arises due to the asymmetric dislocation motion is required to generate a second harmonic. Similarly, it may be concluded here that such an asymmetry is also required to generate a static displacement component. It may be further noted that a symmetric dislocation motion would exist only when there are isolated dislocations which are initially pinned by point defects and are initially not bowed. Such a condition would exist for example in an annealed material which has very low dislocation density. For

materials such as those deformed by fatigue, plastic deformation or super plastic deformation dislocation motion and hence an asymmetric dislocation motion would always exist and would contribute to the generation of the second harmonic. Further some of the materials processed using new processes would have ultra-refined grains and hence there would be an additional stress caused by the dislocations in the cell walls which form grain sub-boundaries. These would generate additional image stresses on the dislocation in addition to the dislocations accumulated within the cell. These image stresses would further increase the asymmetry in dislocation motion.

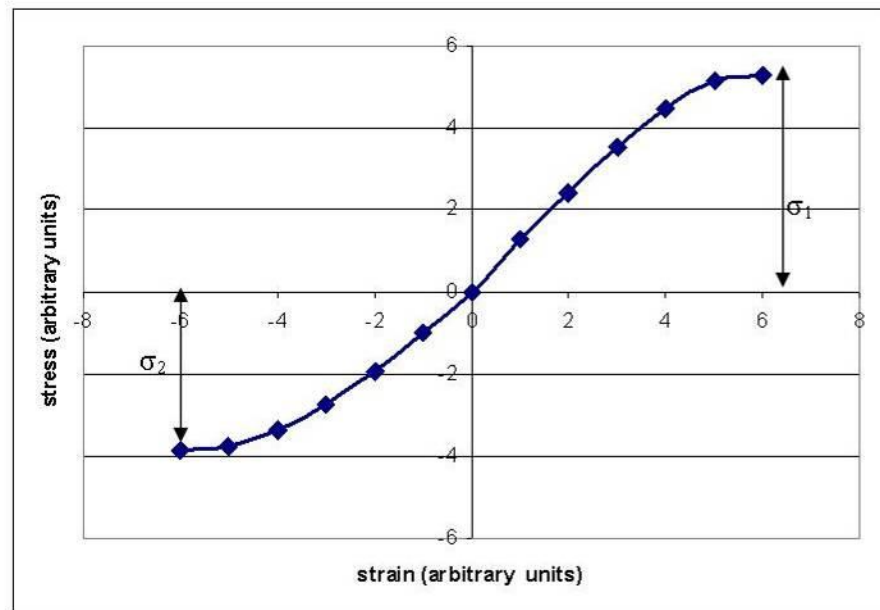


Fig 6. A typical asymmetric stress-strain curve

1.3.1 Dependence of the static displacement component on various input parameters

The dependence of the static displacement component on the following input parameters was explored

(a) The nonlinearity parameter of the material

Fig 8 shows the variation of the static displacement component with the nonlinearity parameter β (usually measured using the amplitude of the 2nd harmonic that is generated when the ultrasonic wave passes through a non-linear material) of the material for different distances of propagation for $\omega=5MHz$ and $A_I=10nm$. It was again observed that the static displacement component varies linearly with the nonlinearity parameter β of the material for all the distances of propagation.

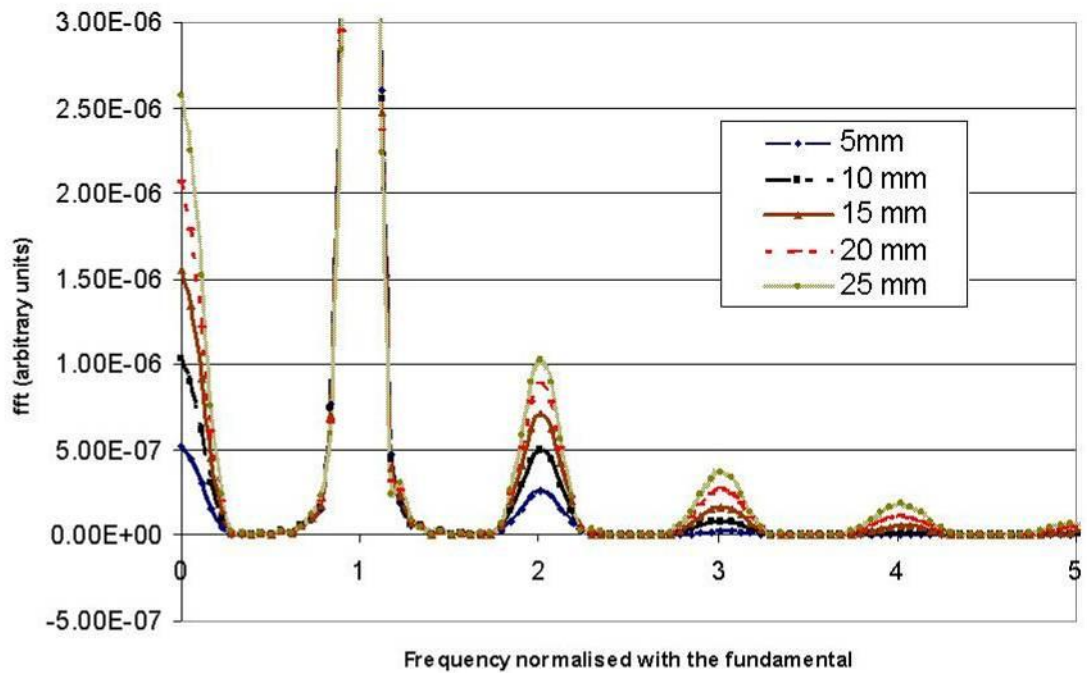


Fig 7. FFT of the propagated wave for Case II after different distances of propagation showing a generated static displacement component.

(b) *The frequency of the input wave*

Fig 9 shows the variation of the static displacement component with the frequency of the input wave for different distances of propagation for $\beta=16$ and $A_I=10nm$.

From the least square fit it can be seen that the static displacement component varies as the square of the frequency of the input wave for all the distances of propagation.

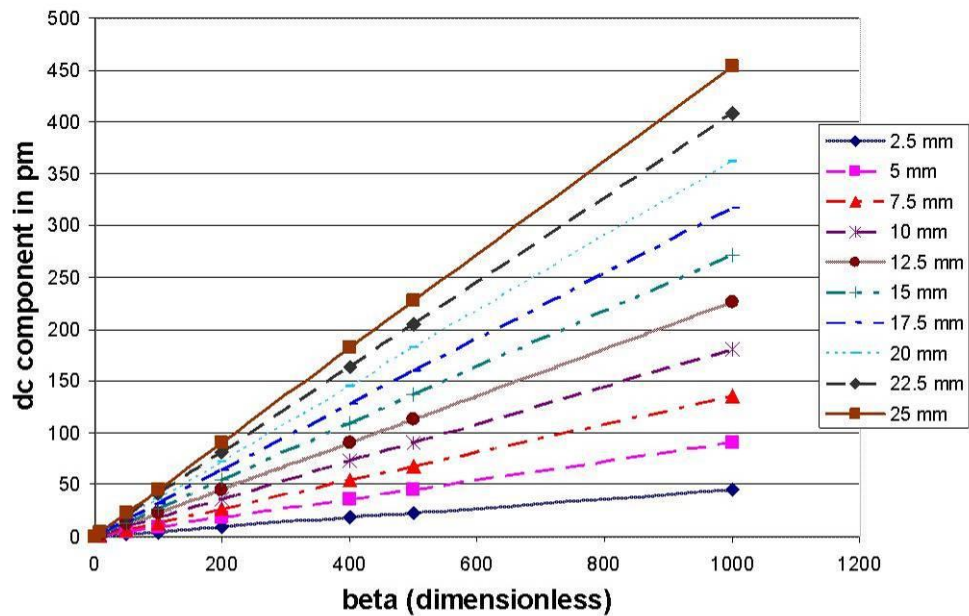


Fig 8. Variation of the static displacement component with the nonlinearity parameter for different distances of propagation for $\omega = 5\text{MHz}$, $A_1 = 10\text{nm}$.

(c) *The amplitude of the input wave*

Fig 10 shows the variation of the static displacement component with the amplitude of the input wave for different distances of propagation for $\omega = 5\text{MHz}$ and $\beta = 16$. From least square fit it can be seen that the static displacement component varies as the square of the amplitude of the input wave for all the distances of propagation.

(d) *The distance of propagation*

Fig 11 shows the variation of the static displacement component with the distance of propagation for various input amplitudes for $\omega = 5\text{MHz}$ and $\beta = 16$. It was observed that the static displacement component varies linearly with the distance of propagation.

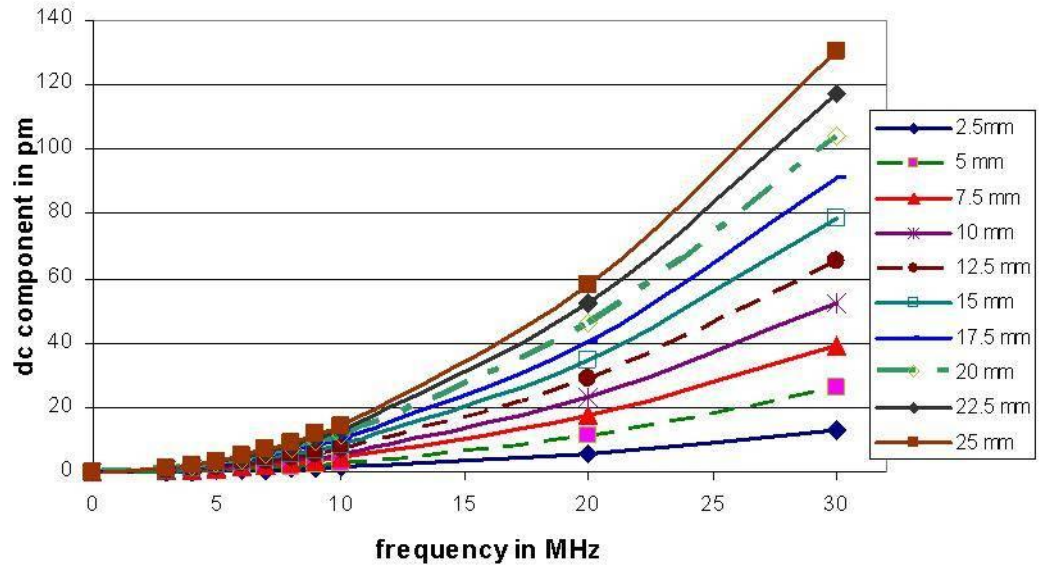


Fig 9. Variation of the static displacement component with frequency for different distances of propagation for $\beta = 16, A_1 = 10nm$.

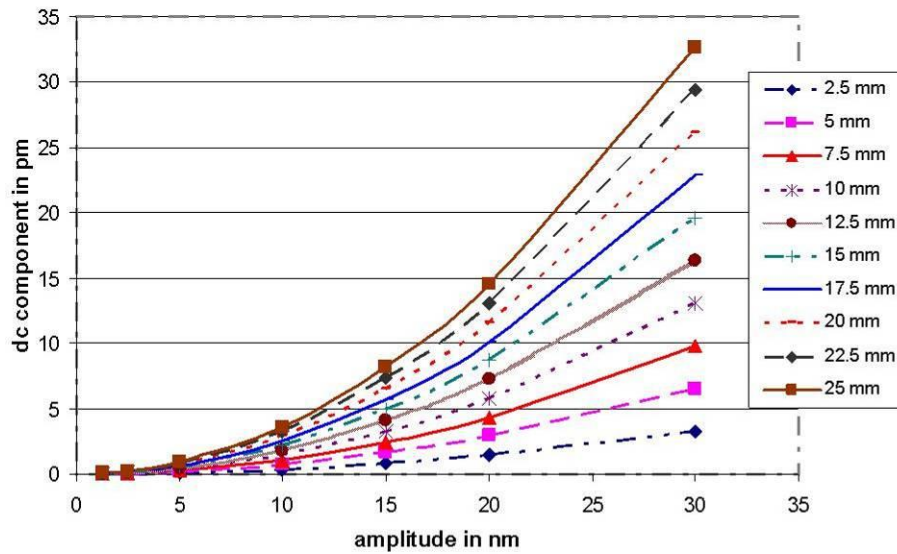


Fig 10. Variation of the static displacement component with the amplitude of the input wave for different distances of propagation for an input wave of frequency

$$\omega = 5MHz, \beta = 16.$$

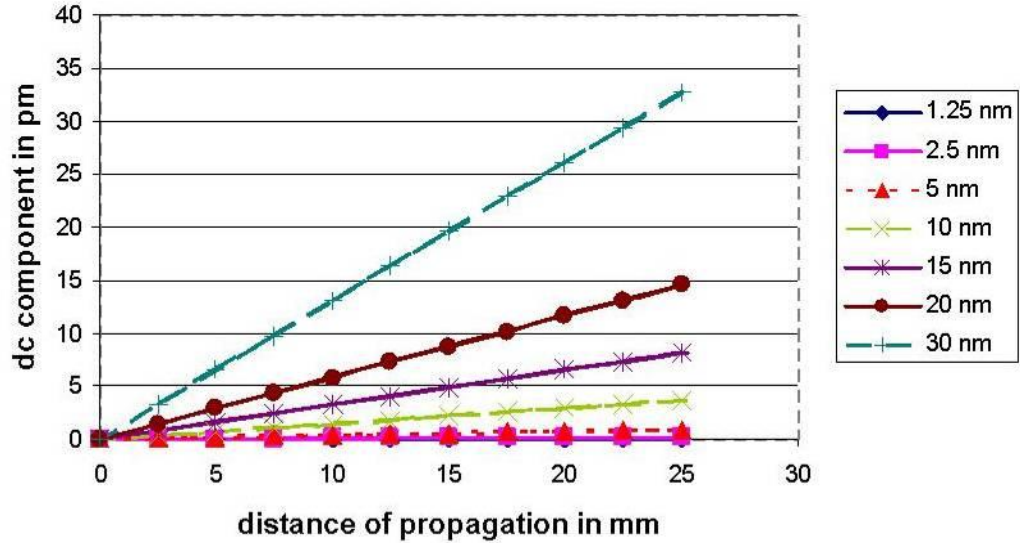


Fig 11. Variation of the static displacement component with the distance of propagation for different input amplitudes for an input wave of frequency $\omega = 5MHz, \beta = 16$

1.4 2D ULTRASONIC WAVE PROPAGATION MODEL FOR MSLM

Mass Spring lattice Model is one among the numerical simulation technique for modeling, simulating and visualizing elastic wave phenomena by discretizing the material into a collection of masses interconnected by springs. In the model two types of springs, linear and torsional are present. This is well illustrated in Fig. 12.

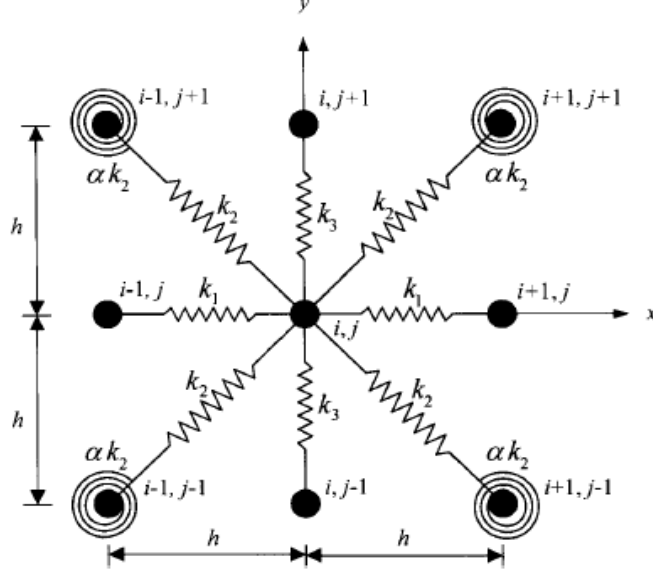


Fig 12. Schematic of a 2D MSLM Model.

1.5 THE 2D MSLM MODEL

The equation of motion for the centre of mass in the x and y direction can be written as

$$\begin{aligned}
 \rho(u_{i,j}^{k+1} + u_{i,j}^{k-1} - 2u_{i,j}^k)/(\Delta t^2) &= F_x + k_1(u_{i+1,j}^k + u_{i-1,j}^k - 2u_{i,j}^k)/h^2 + k_2(u_{i+1,j+1}^k + u_{i+1,j-1}^k + u_{i-1,j+1}^k \\
 &+ u_{i-1,j-1}^k - 4u_{i,j}^k)/2h^2 + k_2\beta(u_{i+1,j+1}^k + u_{i+1,j-1}^k + u_{i-1,j+1}^k + u_{i-1,j-1}^k - 4u_{i,j}^k)/2h^2 + k_2(v_{i+1,j+1}^k \\
 &- v_{i+1,j-1}^k - v_{i-1,j+1}^k + v_{i-1,j-1}^k - 4u_{i,j}^k)/2h^2 + k_2\beta(-v_{i+1,j+1}^k + v_{i+1,j-1}^k + v_{i-1,j+1}^k - v_{i-1,j-1}^k - 4u_{i,j}^k)/2h^2 \\
 \\
 \rho(v_{i,j}^{k+1} + v_{i,j}^{k-1} - 2v_{i,j}^k)/(\Delta t^2) &= F_y + k_3(v_{i+1,j}^k + v_{i-1,j}^k - 2v_{i,j}^k)/h^2 + k_2(v_{i+1,j+1}^k + v_{i+1,j-1}^k + v_{i-1,j+1}^k \\
 &+ v_{i-1,j-1}^k - 4v_{i,j}^k)/2h^2 + k_2\beta(v_{i+1,j+1}^k + v_{i+1,j-1}^k + v_{i-1,j+1}^k + v_{i-1,j-1}^k - 4v_{i,j}^k)/2h^2 + k_2(u_{i+1,j+1}^k - u_{i+1,j-1}^k \\
 &- u_{i-1,j+1}^k + u_{i-1,j-1}^k - 4u_{i,j}^k)/2h^2 + k_2\beta(-u_{i+1,j+1}^k + u_{i+1,j-1}^k + u_{i-1,j+1}^k - u_{i-1,j-1}^k - 4u_{i,j}^k)/2h^2
 \end{aligned}
 \tag{11}$$

where $u_{i,j}^k$ and $v_{i,j}^k$ denote the x and y displacements on the mass particle at the position (i, j) and at the time $t = k\Delta t$, where Δt is the time step; k_1 , k_2 , k_3 , and α are the stiffnesses. β can be expressed as $\beta = \alpha/(2h^2)$.

The wave equations in plain strain transverse isotropic elastic medium is

$$\left. \begin{aligned} \rho \left(\frac{\partial^2 u}{\partial t^2} \right) &= C_{11} \left(\frac{\partial^2 u}{\partial x^2} \right) + (C_{12} + C_{33}) \left(\frac{\partial^2 v}{\partial x \partial y} \right) + C_{33} \left(\frac{\partial^2 u}{\partial y^2} \right) + F_x \\ \rho \left(\frac{\partial^2 v}{\partial t^2} \right) &= C_{22} \left(\frac{\partial^2 v}{\partial y^2} \right) + (C_{12} + C_{33}) \left(\frac{\partial^2 u}{\partial x \partial y} \right) + C_{33} \left(\frac{\partial^2 v}{\partial x^2} \right) + F_y \end{aligned} \right\} \text{-----(12)}$$

where u and v are the displacement in the x and y direction respectively,

ρ is the mass density of the medium, C_{ij} are the elements of stiffness matrix. For isotropic materials C_{ij} are expressed in terms of the Lamé's constant λ and μ as

$$C_{11} = C_{22} = \lambda + \mu, \quad C_{33} = \mu \quad \text{and} \quad C_{12} = \lambda.$$

After discretizing the above equation using center difference method and as the LHS of two equations are equal, RHS can be equated, then we get

$$k_1 = C_{11} - C_{33}, \quad k_3 = \frac{3C_{33} + C_{12}}{4}, \quad k_3 = C_{22} - C_{33}, \quad \text{and} \quad \beta = \frac{C_{33} - C_{12}}{3C_{33} + C_{12}} \text{ for transversely}$$

$$\text{isotropic material and } k_1 = k_3 = \lambda + \mu, \quad k_2 = \frac{\lambda + 3\mu}{4} \quad \text{and} \quad \beta = \frac{\mu - \lambda}{\lambda + 3\mu} \text{ for isotropic media}$$

From the first set of equations the displacement for the (k+1)th time step can be determined from the displacement values of kth and (k-1)th time step as follows.

$$\begin{aligned} (u_{i,j}^{k+1} &= -u_{i,j}^{k-1} + 2u_{i,j}^k + F_x / \rho(\Delta t^2) + k_1(u_{i+1,j}^k + u_{i-1,j}^k - 2u_{i,j}^k) / \rho(\Delta t^2) h^2 + k_2(u_{i+1,j+1}^k + u_{i+1,j-1}^k + u_{i-1,j+1}^k \\ &+ u_{i-1,j-1}^k - 4u_{i,j}^k) / \rho(\Delta t^2) 2h^2 + k_2 \beta (u_{i+1,j+1}^k + u_{i+1,j-1}^k + u_{i-1,j+1}^k + u_{i-1,j-1}^k - 4u_{i,j}^k) / \rho(\Delta t^2) 2h^2 + k_2 (v_{i+1,j+1}^k \\ &- v_{i+1,j-1}^k - v_{i-1,j+1}^k + v_{i-1,j-1}^k - 4u_{i,j}^k) / \rho(\Delta t^2) 2h^2 + k_2 \beta (-v_{i+1,j+1}^k + v_{i+1,j-1}^k + v_{i-1,j+1}^k - v_{i-1,j-1}^k - 4u_{i,j}^k) / \rho(\Delta t^2) 2h^2 \end{aligned}$$

$$\begin{aligned}
(v_{i,j}^{k+1} = -v_{i,j}^{k-1} + 2v_{i,j}^k = F_y / \rho(\Delta t^2) + k_3(v_{i+1,j}^k + v_{i-1,j}^k - 2v_{i,j}^k) / \rho(\Delta t^2)h^2 + k_2(v_{i+1,j+1}^k + v_{i+1,j-1}^k + v_{i-1,j+1}^k \\
+ v_{i-1,j-1}^k - 4v_{i,j}^k) / \rho(\Delta t^2)2h^2 + k_2\beta(v_{i+1,j+1}^k + v_{i+1,j-1}^k + v_{i-1,j+1}^k + v_{i-1,j-1}^k - 4v_{i,j}^k) / \rho(\Delta t^2)2h^2 + k_2(u_{i+1,j+1}^k - u_{i+1,j-1}^k \\
- u_{i-1,j+1}^k + u_{i-1,j-1}^k - 4u_{i,j}^k) / \rho(\Delta t^2)2h^2 + k_2\beta(-u_{i+1,j+1}^k + u_{i+1,j-1}^k + u_{i-1,j+1}^k - u_{i-1,j-1}^k - 4u_{i,j}^k) / \rho(\Delta t^2)2h^2
\end{aligned}$$

where h is the space step (grid size) and Δt is the ime step.

Element size and time step determination

To accurately model the wave, there should be at least 8 elements within the minimum wavelength. Minimum wavelength is for shear wave and hence for the present case the grid size is taken as

$$h = \frac{\lambda_{\min}}{16} \text{ and } \lambda_{\min} = \frac{C_s}{f},$$

where λ is the wave length C_s is the shear velocity in solid and f is the frequency. The shear wave velocity can be obtained from the material parameters E and Poisson's ratio as

$$C_s = \frac{E}{2\rho(1+\nu)}.$$

For a stable wave to propagate through the explicit numerical scheme the Courant number, $\frac{C\Delta t}{h} \leq 1$, where C is the longitudinal wave velocity. Hence the time increment

$$\text{is taken as } dt = \frac{h}{\sqrt{2}C},$$

$$\text{where } C = \frac{E(1-\nu)}{\rho(1+\nu)(1-2\nu)}$$

As per Hyunjune and Younghoon (2000), after a critical value of 1.6937×10^{-4} for $\frac{\Delta t}{h}$, the numerical scheme is not stable. For our particular case it is 1.3964×10^{-4} . So stability condition is met with the present MSLM.

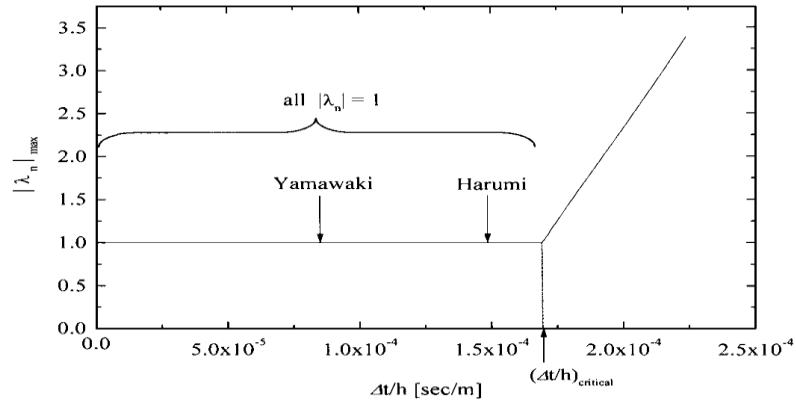


Fig. 13. The selection of critical values using as per Hyunjune and Younghoon (2000)

1.6 2D MSLM SIMULATION RESULTS USING MATLAB

Material selected for the simulation is steel with density 7800 kg/m^3 , Poisson's ratio 0.3 and Young's modulus 200 MPa. The material is considered as a collection of masses and spring and a MATLAB code was written for finding the displacement in the x and y direction for the equation of motion.

Figure .14a, shows the wave propagation when a single cycle sine pulse was given at the centre and imposing rigid boundary condition. Both longitudinal and shear waves can be seen. When the excitation was given at the surface Fig.14b, surface waves are absent with rigid boundary condition.

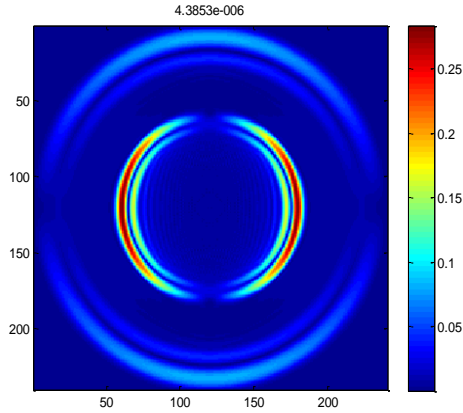


Fig.14a.Source at the centre

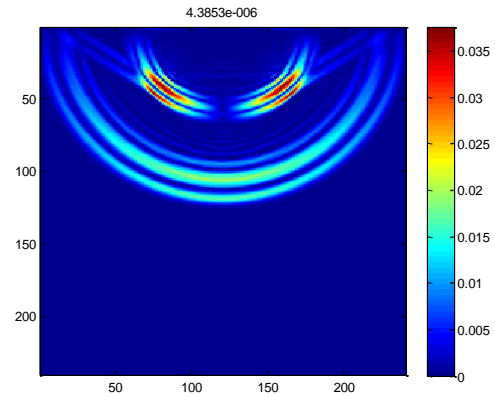


Fig.14b Source at the surface

For the proper visualization of free surface condition, equations are written separately for the nodes along the boundary and at the corners. Along the boundary masses and springs are halved and at the corners only $\frac{1}{4}$ th mass is taken. After incorporating the above condition surface wave could also be seen in addition to longitudinal and shear waves as shown in Fig 15.

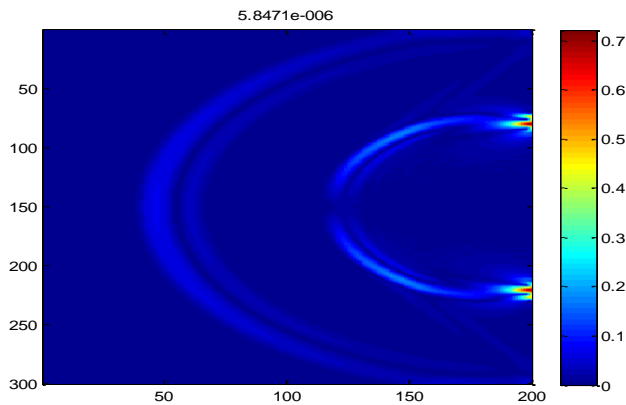


Fig. 15. The visualization of both L and S waves using MSLM 2D model.

Later code was modified by, giving frequency, number of cycles and dimensions of the specimen as input. The results for a 3 cycle 100 kHz hanning windowed pulse is shown below for different time intervals after the initial pulse was applied on the surface..

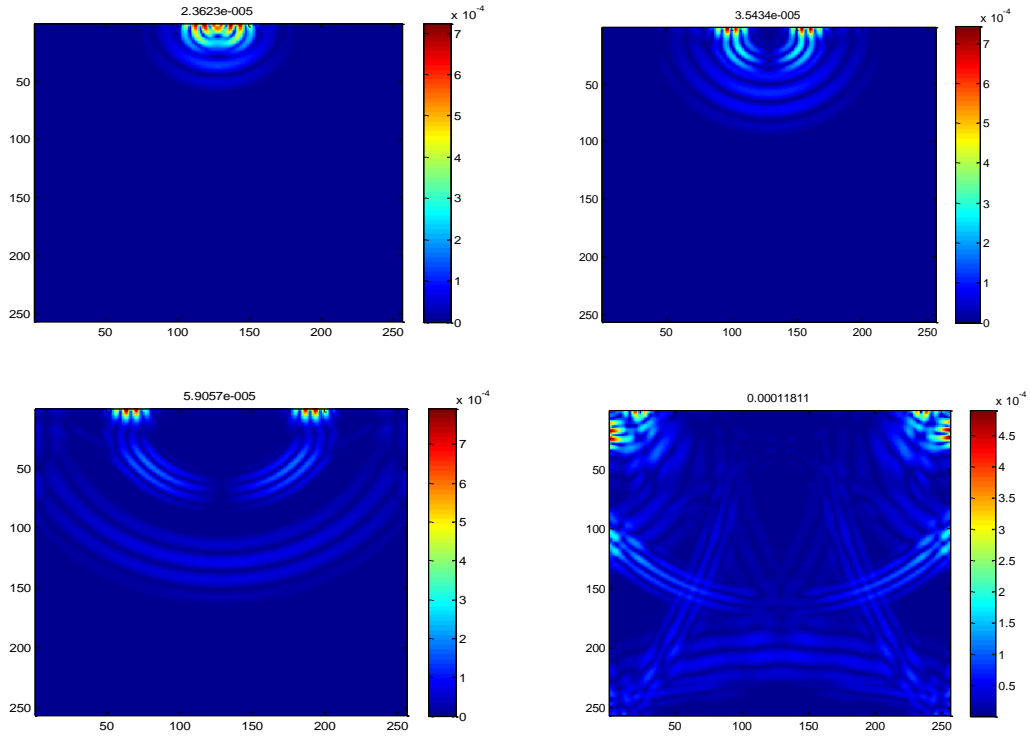


Fig. 16. The 2D visualization of wave propagation in a 2D isotropic media at different time intervals using the MSLM model.

‘A’ scans at different points were also plotted as shown in Fig. 17 at discrete points in the 2D media.

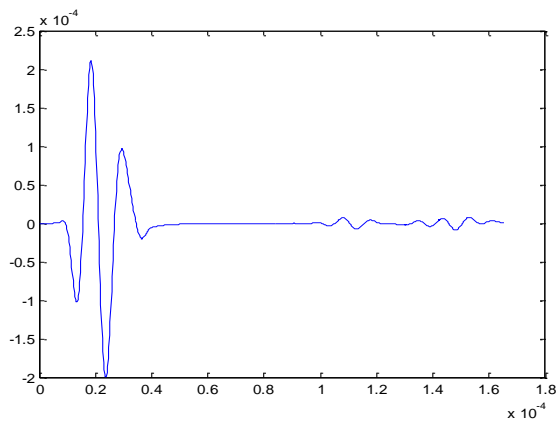
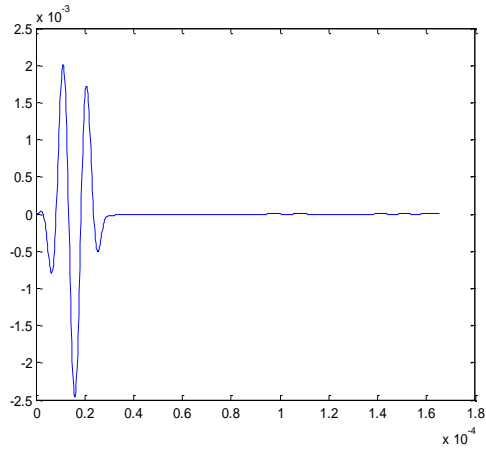
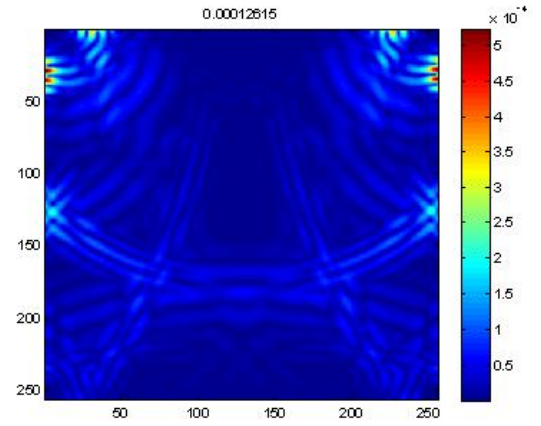
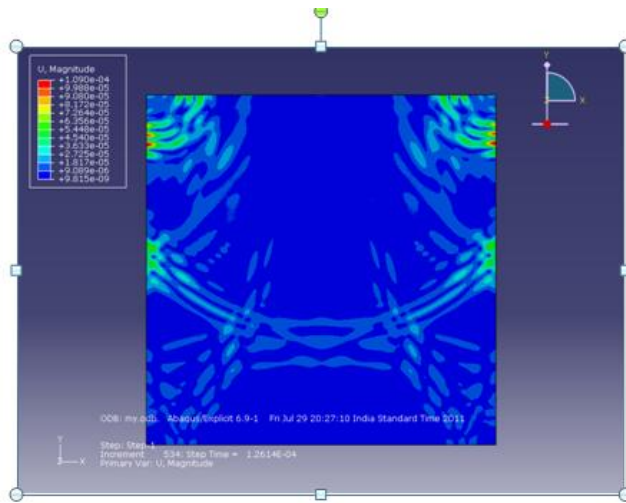
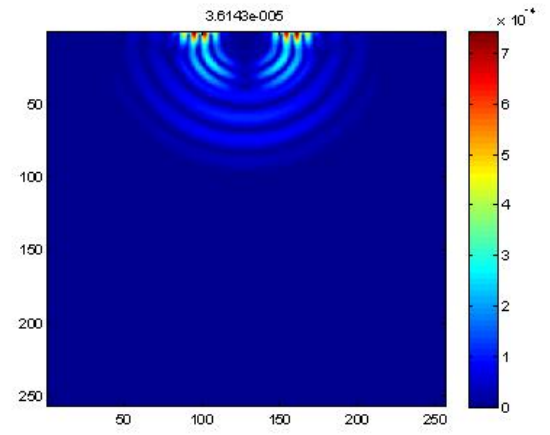
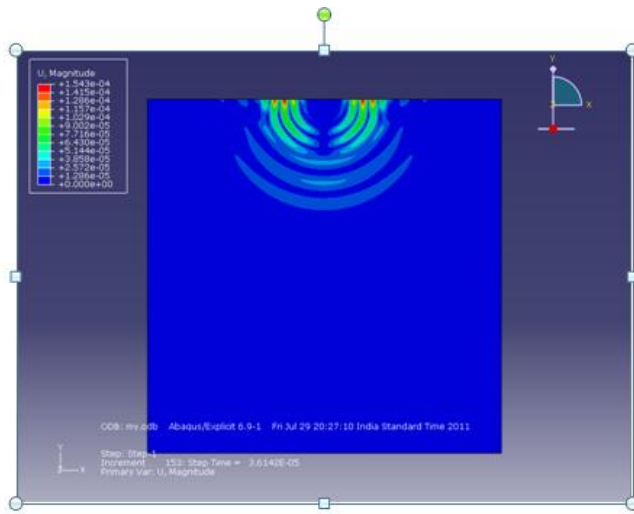


Fig.17 A scans at different points.(a).At the source point(1,128) (b) At (50,128) (c)At (80,128) and (d)At (128,128)

1.7 COMPARISON WITH COMMERCIAL FEM SOFTWARE (ABAQUS).

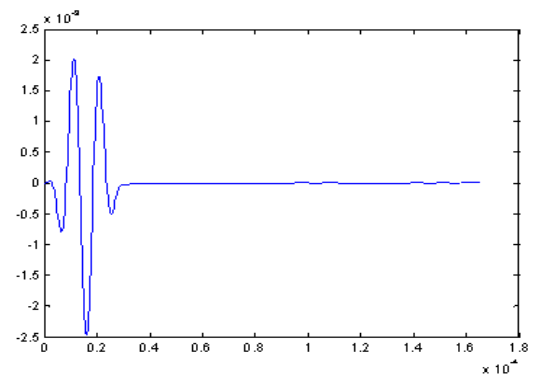
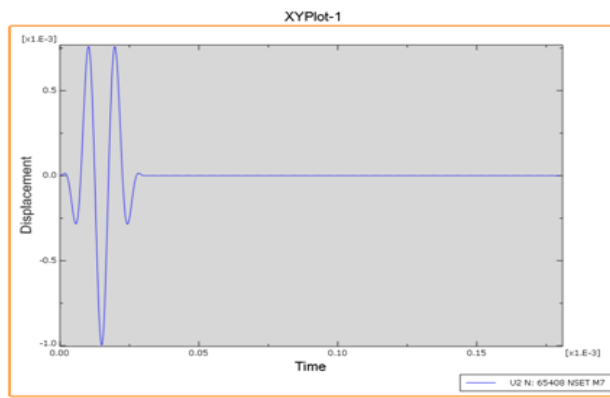
Results obtained with MSLM are compared with the results obtained from Abaqus in which the same source was given as the input. The wave propagation simulation plots are provided in the form of color images at different time intervals in Fig.18. The plots with GREY background are results obtained using ABAQUS while the plots with WHITE background represent the MSLM model results in Fig. 19.



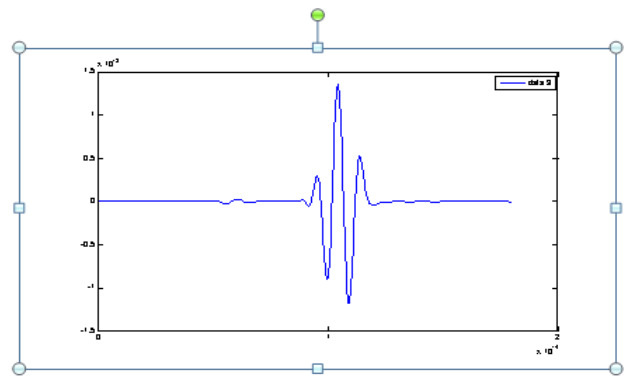
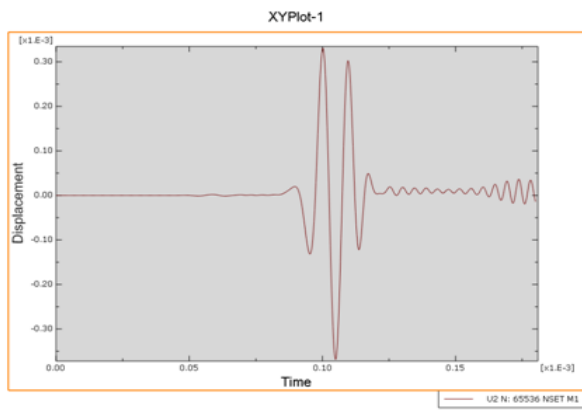
(a) ABAQUS FEM MODEL

(b) MSLM MODEL

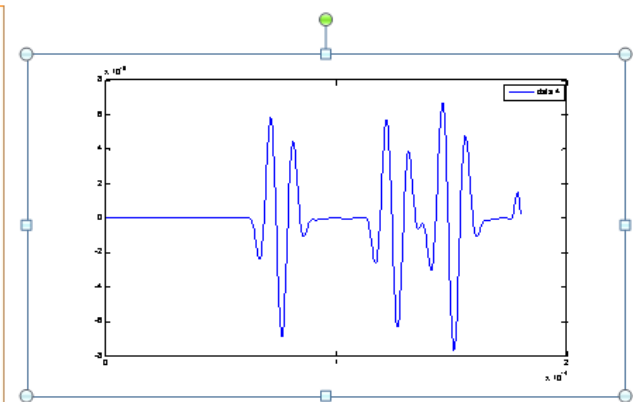
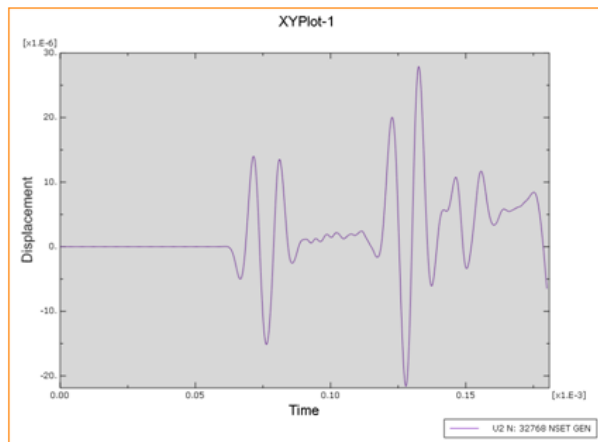
Fig. 18. The simulation of the wave propagation using ABAQUS FEM model for a points source in a 2D domain at 2 different time intervals, using (a) ABAQUS and (b) MSLM Model developed in MATLAB.



(a) At the source point



(b) At the right corner



(c) At the right edge middle point

Fig. 19. The A-scan signals at different points as obtained from ABAQUS and MSLM models.

It is concluded from these results that the 2D MSLM model developed using MATLAB, developed in this project compares well with the 2D ABAQUS FEM model that is commercially available. Hence, the validity of the MSLM model for linear ultrasonic wave propagation is validated herewith. The advantage of the MSLM model, over commercially available FEM models includes (a) The ability to model the mechanics of the wave propagation at micron scales, and (b) The ability to introduce non-linear behavior of the springs, which can be used to simulate NLU parameters for the current studies.

1.8 FUTURE WORK IN 2D MSLM MODELLING

It is planned to introduce non-linear behavior of the individual components of the MSLM model in order to simulate NLU behavior, as was earlier demonstrated in the 1D case. Once this is developed, the 3D version will be developed for the improved understanding of the NLU behavior in materials.

1.9 REFERENCES

Balasubramaniam K., Valluri J. S., and Prakash R. V., Creep damage characterization using a low-amplitude nonlinear ultrasonic technique, to appear in *Materials Characterisation* (2011)

Bermes C., Jin-Yeon K., Qu J. and Jacobs L. J. (2007), Experimental Characterization of Material Nonlinearity using Lamb Waves, *Applied Physics Letters* 90, 021901

Cantrell J. H. (1984), Acoustic Radiation Stresses in Solids, *Physical Review B*, Vol. 30 Number 6

Cantrell J. H., Jr., and Winfree W. P., (1984) Acoustic Radiation Stresses in Solids, *Physical Review B*, Vol. 30 Number 6,

Cantrell J. H. and Yost W.T., (1997) Effect of Precipitate Coherency Strains on Acoustic Harmonic Generation, *J. Appl. Phys.*, Vol. 81, No. 7

Cantrell J. H., and Yost W. T., (2001) Nonlinear Ultrasonic Characterization of Fatigue Microstructures, *International Journal of Fatigue* 23 S487–S490

- Cantrell J H.**, (2004) Substructural Organization, Dislocation Plasticity and Harmonic Generation in Cyclically Stressed Wavy Slip Metals, *Mathematical, Physical and Engineering Sciences*, Vol. 460, No. 2043, pp. 757-780
- Cantrell J. H.**, (2006) Quantitative Assessment of Fatigue Damage Accumulation in Wavy Slip Metals from Acoustic Harmonic Generation, *Philosophical Magazine*, Vol. 86, No. 11, 1539–1554,
- Cantrell J. H.**, (2008) Effects of Diffraction and Dispersion on Acoustic Radiation Induced Static Pulses, *Applied Physics Letters* 92, 231914
- Cantrell J H.**, (2009) Nonlinear Dislocation Dynamics at Ultrasonic Frequencies, *Journal of Applied Physics* 105, 043520,
- Hikata A., Chick B. B., and Elbaum C.**, (1965) Dislocation Contribution to the Second Harmonic Generation of ultrasonic waves, *Journal of Applied Physics* Vol. 36 Number1
- Hikata A. and Elbaum C.**, (1966) Generation of Ultrasonic Second and Third Harmonic due to Dislocations I, *Physical Review* Vol. 144 Number2
- Harumi K.**, (1986) Computer Simulation of Ultrasonics in Solids, *NDT International*. Volume 19, No. 5,
- Herrmann J., Kim J., Jacobs. L. J., Qu J., Littles J. W. and Savage M. F.**, (2006) Assessment of Material Damage in a Nickel-base Superalloy using Nonlinear Rayleigh Surface Waves, *Journal of Applied Physics* 99, 124913
- Hurley D. C., Balzar D., Purtscher P. T., and Hollman K. W.**, (1998) Nonlinear Ultrasonic Parameter in Quenched Martensitic Steels, *Journal of Applied Physics*, Volume 83, No. 9,
- Hyunjune Y. and Younghoon S.**, (2000) Numerical Simulation and Visualization of Elastic Waves Using Mass-Spring Lattice Model, *IEEE transactions on ultrasonics, ferroelectrics, and frequency control*, vol. 47, no. 3
- Jayarao V. V. S., Elankumaran K., Raghu V P., and Balasubramaniam K.**, (2008) Fatigue Damage Characterization using Surface Acoustic Wave Nonlinearity in Aluminum alloy AA7175-T7351, *Journal of Applied Physics*, 104, 1
- Jacobs L. J., Kim J. Y., Jianmin Qu, and Littles J. W.**, (2006) Experimental Characterization of Fatigue Damage in a Nickel-base Superalloy using Nonlinear Ultrasonic Waves, *J. Acoustical Society of America*. [DOI: 10.1121/1.2221557]
- Jacob X., Takatsu R., Barrière C., and Royer D.**, (2006) Experimental Study of the Acoustic Radiation Strain in Solids, *Applied Physics Letters* 88, 134111

- Karthik T. N., Elankumaran K., and Balasubramaniam K.,** (2007) Simplified Experimental Technique to Extract the Acoustic Radiation Induced Static Strain in Solids, *Applied Physics Letters* 91, 134103
- Karthik T.N., Kannan E., and Balasubramaniam K.,** (2009) Issues on the Pulse-width Dependence and the Shape of Acoustic Radiation induced Static Displacement pulses in Solids, *J. Appl. Phys.* 105, 073506
- Kommareddy V., Ramaswamy S., Ganesan B., Oruganti R., Bala R. and Shyamsunder MT,** (2006), Quantification of Fatigue using Nonlinear Ultrasound Measurements, *ECNDT - Fr.1.5.4*
- Kyung Y. J.,** (2009), Nonlinear Ultrasonic Techniques for Nondestructive Assessment of Micro-damage in Material, *International Journal of Precision Engineering and Manufacturing* Vol. 10, No. 1, pp. 123-135
- Jitendra S. V.,** (2009) Creep Damage Characterization of Material Systems using Nonlinear Acoustic Techniques, IIT Madras, Chennai, India, Master of Science *Thesis*
- Nilsson S., Petersson N. A., Sjögreen B., and Kreiss H. O.,** (2006), Accurate and Stable Finite Difference Approximations of the Elastodynamic Equations in Second order formulation, *Journal of Computational Physics*
- Peter Li, W. T. Yost, J. H. Cantrell , and K. Salama,** (1985), Dependence of Acoustic Nonlinearity Parameter on Second Phase Precipitates of Aluminum Alloys, *Ultrasonics Symposium*
- Pruell C., Jin-Yeon K., Qu J. and Jacobs L. J.,** (2007), Evaluation of Plasticity Driven Material Damage using Lamb Waves, *Applied Physics Letters* 91, 231911
- Reynolds A. C. (1978),** Boundary Conditions for the Numerical Solution of Wave Propagation Problems, *Geophysics* Vol. 43, No. 6, P. 109Y-1110
- Schroeder C. T. and Waymond R. Scott,** (1999) Finite Difference Time Domain Model for Elastic waves in the Ground, *International Society for Optical Engineering* vol. 3710 (2), pp. 1361-1372
- Sony B., Kowmudi B. N., Omprakash C. M., Satyanarayana D.V.V., Balasubramaniam K. and Kumara V,** (2008) Creep Damage Assessment in Titanium Alloy using a Nonlinear Ultrasonic Technique, *Scripta Materialia* 59, 818–821
- Thirunavukkarasu S., Rao B.P.C., Jayakumar T., Kalyanasundaram P., Raj B. and Balasubramaniam K.,** (2002) Nonlinear Ultrasonic Method for Material Characteristics, *NDE 2002*, Proc. National Conf. of ISNT.

Thompson R. B. and Tierston H. F., (1977) Harmonic Generation of Longitudinal Elastic Waves, *Journal of Acoustic Society of America*, Vol. 62, No.1

Yost W.T. and Cantrell J. H., (1992) The Effects of Fatigue on Acoustic Nonlinearity in Aluminum Alloys, 1051-0117/92/0000-09 *IEEE Trans.*